DOI: 10.13009/EUCASS2019-311

8TH EUROPEAN CONFERENCE FOR AERONAUTICS AND AEROSPACE SCIENCES (EUCASS)

DOI: ADD DOINUMBER HERE

Investigation of RANS turbulence models for cryogenic rocket combustion chambers

Stefan Fechter[⋆†], *Tim Horchler*[⋆], *Sebastian Karl*[⋆] *and Klaus Hannemann*[⋆]
[⋆] *German Aerospace Center (DLR)*
Institute of Aerodynamics and Flow Technology, Spacecraft Department
Bunsenstr. 10, 37073 Göttingen, Germany
stefan.fechter@dlr.de · tim.horchler@dlr.de · sebastian.karl@dlr.de · klaus.hannemann@dlr.de
[†]Corresponding author

Abstract

The accurate numerical simulation of high-pressure rocket combustion chambers is a key element for the design of future space transportation vehicles. The main challenges include the consistent approximation of thermodynamic effects within a broad temperature range. Another open question is which are the additional physical processes that have to be modeled for Reynolds Averaged Navier-Stokes (RANS) based approaches. To this open question we contribute with a detailed study of RANS turbulence models and their influence onto the flame shape for a simplified academic test case and a subscale rocket combustion chamber at supercritical pressure.

1. Introduction

The accurate numerical simulation of jet atomization and high-pressure combustion effects at cryogenic temperatures in rocket combustion chambers is a key element for the design of future space transportation vehicles. One major challenge is to correctly predict the flow field, the non-linear mixing processes, as well as the combustion of the cryogenic fuels. This is needed to estimate the thermal loads onto the combustion chambers walls of future reusable rocket systems by means of a validated based numerical methods for industrial applications. The focus of this contribution is on the development and assessment of different RANS turbulence models, ranging from a simple Spalart-Alamaras turbulence model up to a state of the art Reynolds Shear Stress Model (RSM). Still nowadays higher resolved LES or DES simulation techniques are solely feasible for detailed investigations of simplified rocket combustion chambers. State of the art rocket engines, like the Ariane 5 Vulcain 2 engine, have more than 500 injectors. To be able to investigate detailed, industry-relevant configurations high-fidelity RANS methods are necessary that are able to provide a suitable resolution of the cryogenic high-pressure effects within rocket combustion chambers at trans- or supercritical conditions. This becomes important for investigations of large-scale combustion chambers. Even nowadays, it is impossible with high-resolution methods to simulate full-scale combustion chambers and this will not change in the near future.

In open literature, in the context of numerical prediction of cryogenic injection processes, it is an open question how cryogenic sub- and supercritical injection process, especially within rocket combustion chambers, can be modeled (see e. g. the discussion in Oefelein,[19] Bellan[4]) and especially which physical processes are important to characterize the jet breakup and the phase transition processes correctly. At these conditions all fluid properties have a strong sensitivity to changes of the thermodynamic quantities: All thermodynamic quantities are dependent of the density as well as the temperature. Detailed previous investigations of the thermodynamic structure of LOx-H_2 diffusion flames have been performed by Banuti et al.[3] They showed, based on detailed LES investigations, that non-linear mixture effects are limited to a small area between the phase interface and the flame. This is a region in which the temperature changes from cold injection conditions to high temperatures in the flame zone within few cells. With steady-state RANS methods on a much coarser grid, it is impossible to resolve such fine segments at the phase interface. An open question is whether this small transition region close to the phase boundary has an effect on the overall pressure and thermal loads prediction of the combustion chamber; questions that are typically addressed using RANS-based methods.

DOI: 10.13009/EUCASS2019-311

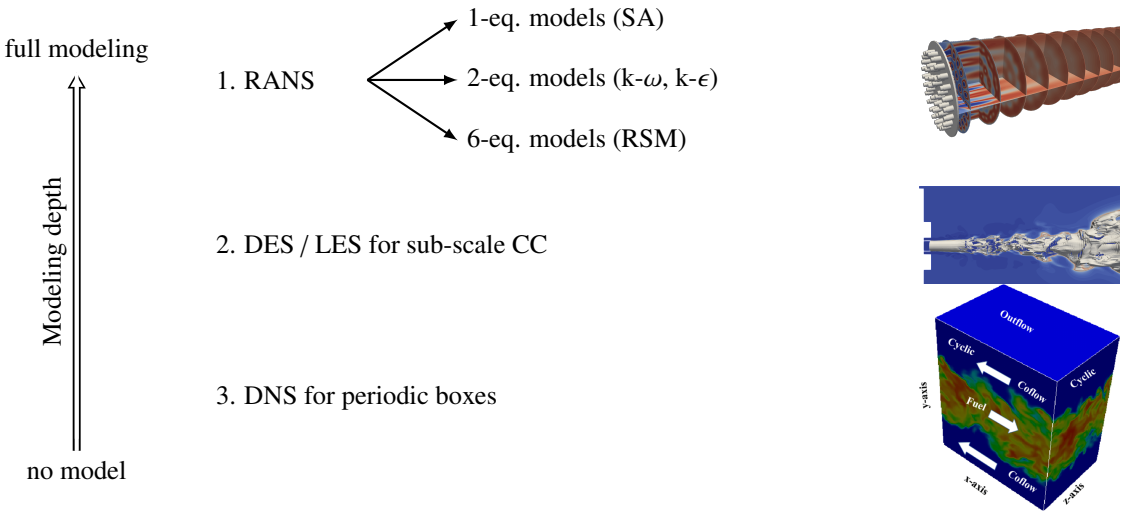

Figure 1: Numerical methods to resolve or model turbulence effects

The focus of this paper is on the modeling of the turbulent effects within cryogenic rocket combustion chambers. We begin this investigation by looking into the thermodynamic and physic effects for this kind of flows: According to a detailed flamelet-based study of Banuti et al.[3] the flame structure within a LOx-H_2 diffusion flame is characterized by an anchored flame at the injector outlet and a small region with non-ideal mixture of the liquid oxygen and the burned gases close to the flame. Within high-resolved detailed LES/DES investigations the flame gets a turbulent structure and the non-linear mixture effects play an important role. Within RANS-based approaches only the mean flame topology is resolved resulting in a thicker flame front. Several approaches exist to include the turbulence-combustion interaction effects within the RANS methods, e. g. by Probability Density Function (PDF) methods (see e. g. description in the book of Gerlinger[8]). However, even this thickened averaged flame zone can not be resolved detailed and the effects of this small layer with a strong density and temperature gradient in the flame zone has to be modeled within the RANS turbulence model. The aim of this study is to investigate the suitability of two-equation turbulence models (here the Menter SST turbulence model) and Reynolds Shear Stress Models (RSM) for the application within rocket combustion chambers at cryogenic conditions.

Within this topic, another topic is related to the applicability of simplified thermodynamic mixture approximations. This is discussed in the context of the Multi-Fluid mixing model (Banuti et al.[2]) and its efficient implementation based on quadtree tabulation (see Fechter et al.[7] based on the ideas of Dumbser et al.[6]). For this study we use standard cubic equation of states (EOS) to be able to resolve all non-linear mixture effects. To improve the poor density predictions for liquid states, a density correction according to Peneloux et al.[20] is applied.

The study in this paper is structured as follows: In the next section the numerical and thermodynamic model used for the simulation of cryogenic rocket combustion models is discussed. In the following section we validate our RANS turbulence modeling approach to high-resolved LES simulations of the Ruiz test case (see description in Ruiz et al.[25]) for which reference results are available in literature. As a next step we apply this framework to a subscale rocket combustion chamber test case at a supercritical load point for which experimental results are available (see experimental results in Suslov et al.[27,28]).

2. Numerical approach

In this Section we describe the numerical methodology as well as the physical models needed to describe compressible flows within cryogenic rocket chambers at high pressure conditions. A general description is given in the next part while a detailed description of the thermodynamic EOS mixture model at cryogenic injection conditions is given thereafter. A numerical method to suppress spurious numerical oscillations, the Double Flux model (Abgrall & Karni[1] and its application to cryogenic flows in Ma et al.[16]), is detailed in section 2.3.

2.1 Flow solver

The flow solver is the DLR TAU Code for the compressible Navier-Stokes equations with various RANS turbulence models. Only a brief overview is given here, detailed descriptions can be found in Hannemann,[10] and Karl.[13] TAU is

DOI: 10.13009/EUCASS2019-311

No.	Reaction			Rate Constants A	n	E
1	$H_2 + O_2$	$\rightleftharpoons$	$HO_2 + H$	1.0000e+14	0.00	5.6000e+04
2	$H + O_2$	$\rightleftharpoons$	$HO + O$	2.6000e+14	0.00	1.6800e+04
3	$O + H_2$	$\rightleftharpoons$	$HO + H$	1.8000e+10	1.00	8.9000e+03
4	$HO + H_2$	$\rightleftharpoons$	$H_2O + H$	2.2000e+13	0.00	5.1500e+03
5	$2\,HO$	$\rightleftharpoons$	$H_2O + O$	6.3000e+12	0.00	1.0900e+03
6[1]	$H + HO + M$	$\rightleftharpoons$	$H_2O + M$	2.2000e+22	-2.00	0.0000e+00
7[2]	$2\,H + M$	$\rightleftharpoons$	$H_2 + M$	6.4000e+17	-1.00	0.0000e+00

Table 1: Simplified Jachimowski hydrogen-oxygen reaction mechanism as detailed in Gerlinger.[8]

a hybrid grid, finite volume, compressible flow solver. It has been verified for a variety of steady and unsteady flow cases, ranging from sub- to hypersonic Mach numbers. Only models relevant for the present work in the area of rocket combustion chamber simulations are discussed in the following.

The mixture of chemically reacting flows governed by the compressible Navier-Stokes equations is solved using a Godunov type finite volume method. Second order spatial accuracy is obtained using MUSCL reconstruction at cell interfaces. The low Mach numbers and high density gradients, which are a challenge for a compressible flow solver, can be dealt with using a MAPS+ Riemann solver by Rossow.[23] We apply the Double Flux model for cryogenic mixtures (see Section 2.3) together with a cubic mixture EOS (see Section 2.2). Within the study of the turbulence effects we apply different turbulent models within the RANS approach: a Spalart-Alamaras turbulence model,[26] a Menter SST model[18] and a Reynolds stress turbulence with a Wilcox stress ω model,[29] that is similar to the well-known Launder-Reece-Rodi model. The Menter baseline omega equation[17] is used to predict the turbulent length and time scale.

In the present work, TAU's finite rate chemistry model is used in thermal equilibrium. Chemical source terms are calculated from Arrhenius' equations, backward reaction rates are calculated using the forward rates and the equilibrium constants. The kinetic mechanism is a simplified Jachimowski's[12] 6 species, 7 reaction model, as reported by Gerlinger[9] (see Table 1). The considered species are H_2, O_2, OH, H_2O, O, H.

The EOS is described by a volume-corrected cubic Peng-Robinson mixture EOS. The corresponding cryogenic high-pressure mixture transport coefficients are estimated using the Chung high-pressure viscosity and heat transfer coefficient correlations, as e. g. described in Poling et al.[22]

2.2 Cryogenic fluid model

Within the transcritical injection process in rocket combustion chambers, in which the oxygen is injected at a subcritical temperature and supercritical pressure. To be able to capture the thermodynamic effects in this region correctly, the fluid mixture is described based on a cubic Peng-Robinson EOS (Peng & Robinson[21]). This is a standard method to describe the thermodynamic behavior of non-ideal cryogenic fluid mixtures. To improve the poor density estimate of standard cubic EOS, a volume shift is added according to the method of Peneloux et al.[20] With this modifications density estimates for the liquid phases are accurate within 3% compared reference-style EOS.

The details of the thermodynamic description are summarized in the appendix (see section Appendix A).

2.3 Double-flux model for cryogenic mixtures

The first ideas to prevent non-physical oscillations in multi-species simulations originate back to Abgrall & Karni[1] and have been further improved by Billet & Abgrall.[5] In both publications the aim was to prevent pressure oscillations within an ideal gas mixture due to spatially varying adiabatic mixture coefficients γ that depend on the local composition. The main idea was to apply non-conservative energy fluxes (a simple Ghost-Fluid method) with a fixed γ during the Runge-Kutta time integration that removed the numerical oscillations. This approach was generalized by Ma et al.[16] for the application within cryogenic real-fluid mixtures, one application in which non-ideal mixture states cause unphysical numerical pressure oscillations. For real-gas flows these oscillations have a much larger influence on the simulation.

Here we sketch briefly the idea of the double-flux model for real-gas flows: In a first step the real-gas mixture state is linearized and a general adiabatic coefficient γ^* (based on the expression for the sound speed of an ideal gas) is

DOI: 10.13009/EUCASS2019-311

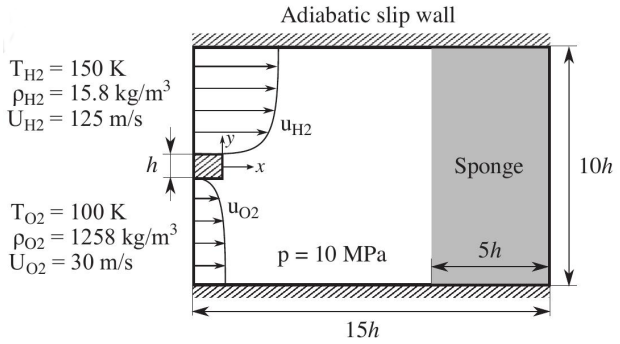

Figure 2: Ruiz test case: domain and inlet conditions

defined for each grid point:

$$\gamma^* = \frac{\rho c^2}{p}. \tag{1}$$

Note that for one ideal gas species, the adiabatic coefficients γ and γ^*, are identical. For a multi-species mixture γ^* will be a nonlinear function of the mixture composition and may not be constant. Similarly we mimic the energy equation for an ideal gas to define an energy offset

$$e_0^* = e - \frac{p}{\rho(\gamma^* - 1)} \tag{2}$$

that is zero for an ideal gas flow. The values for γ^* and e_0^* are kept constant within each Runge-Kunga time step. The fluxes for a cell i are calculated using the specific values for γ_i^* and $e_{0,i}^*$ for the cell resulting in an non-conservative energy formulation. This formulation is designed in that way that the pressure oscillations due to mixing effects are efficiently removed.

3. Validation of numerical approach

For a first validation of the numerical method we choose the Ruiz test case as introduced by Ruiz et al.[25] This test case is a simplified two-dimensional model of a cryogenic injector (half-model of a coaxial injector). The flow conditions (injection temperature and pressure) are chosen such to resemble typical operating conditions of rocket combustion chambers and their usual transcritical injection conditions with subcritical temperature and supercritical pressure (for the oxygen). The domain size just considers the primary atomization processes at the liquid oxygen jet. The domain as well as the inlet conditions are shown in Figure 2. Within the DES approach we use a two-dimensional mesh size of about 0.5 Mio DOF, while for the RANS computations a ten times coarser mesh (about 50 000 DOF) is used.

Reference results for the flow statistics are provided in the paper of Ruiz et al.[25] for a generic 2D LES of the flow field. We apply here our numerical method with a zonal Double-Flux model with a density-gradient based indicator as described in Ma et al.[16] At the end of the domain we apply a sponge zone in which we apply more a dissipative RANS upwind scheme to damp reflections at the outflow boundary condition.

3.1 Mixing test case

In the first case, we just consider a cryogenic (non-ideal) mixing of the liquid oxygen with the gaseous hydrogen that are both described by a cubic Peng-Robinson EOS. A visual plot of the instantaneous flow topology is shown in Figure 3. The statistical evaluation concerning the mean and the root mean square (RMS) fluctuations is shown in the Figures 4-7 at different cut-plane positions in the flow field. In these plots the validation results taken from Ruiz et al.[25] are included.

With the DES approach in TAU we are able to reproduce the mean and rms distributions at the different transverse cuts. The TAU solution is comparable to the reference results given by the AVBP code. Even using the RANS approach on the coarse grid we are able to reproduce the mean flow field at the transverse positions. Note, however, that the RANS solution is not identical to the 2D DES approach, because the two-dimensional RANS provides a physically reasonable turbulence field in contrast to a non-physical turbulence field for the 2D DES/LES approach. Because of that some minor deviations in the mean flow variables can be seen in the magnitude of the mean velocity peaks in the transverse cuts (see Figures 4-7).

DOI: 10.13009/EUCASS2019-311

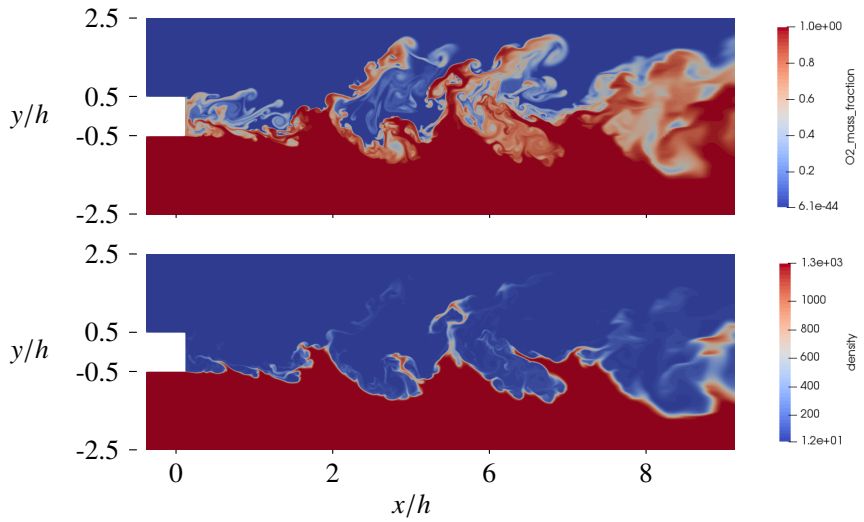

Figure 3: Instantaneous fields of oxygen mass fraction, and density from top to bottom for the two-dimensional LOX/GH2 mixing case.

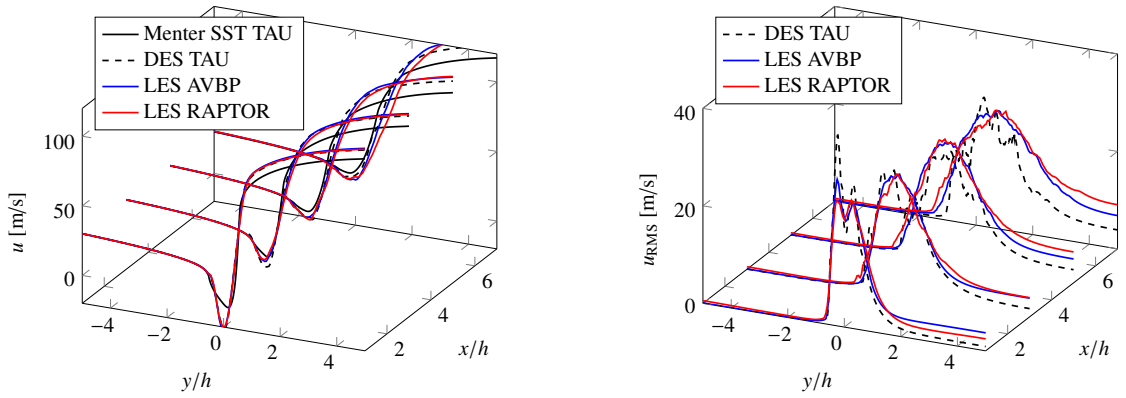

Figure 4: Transverse cuts of (a) mean and (b) rms axial velocity of the two-dimensional LOX/GH2 mixing case.

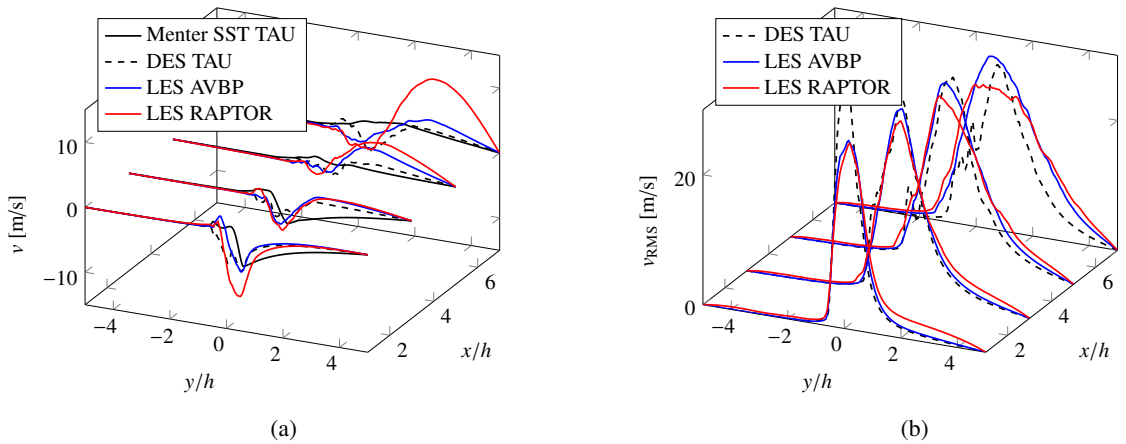

Figure 5: Transverse cuts of (a) mean and (b) rms transverse velocity of the two-dimensional LOX/GH2 mixing case.

DOI: 10.13009/EUCASS2019-311

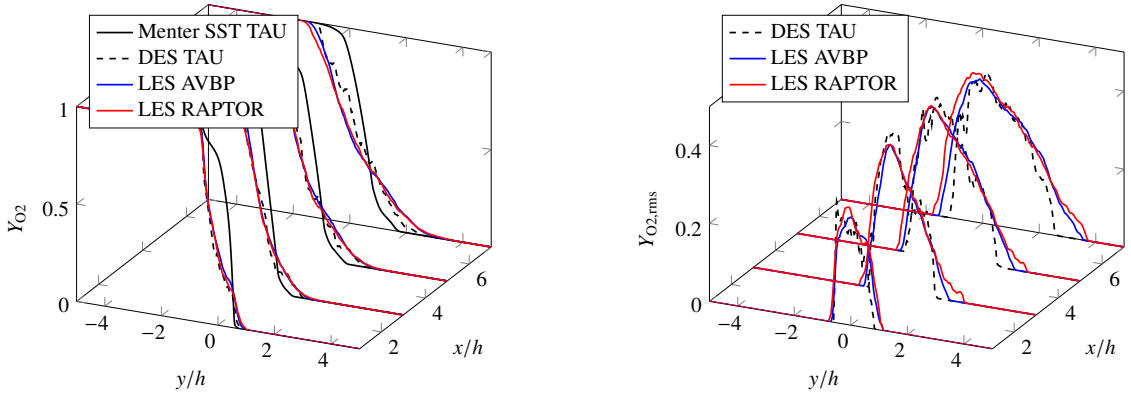

(a) (b)

Figure 6: Transverse cuts of (a) mean and (b) rms oxygen mass fraction of the two-dimensional LOX/GH2 mixing case.

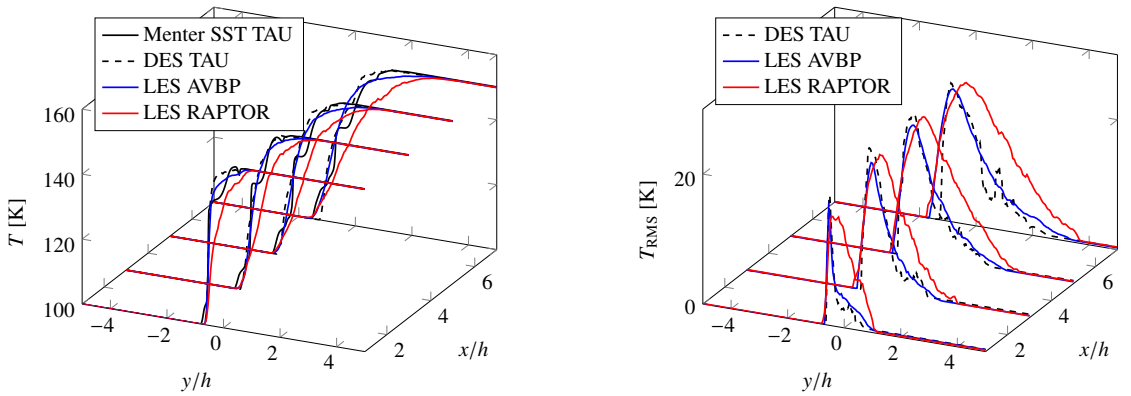

(a) (b)

Figure 7: Transverse cuts of (a) mean and (b) rms temperature of the two-dimensional LOX/GH2 mixing case.

DOI: 10.13009/EUCASS2019-311

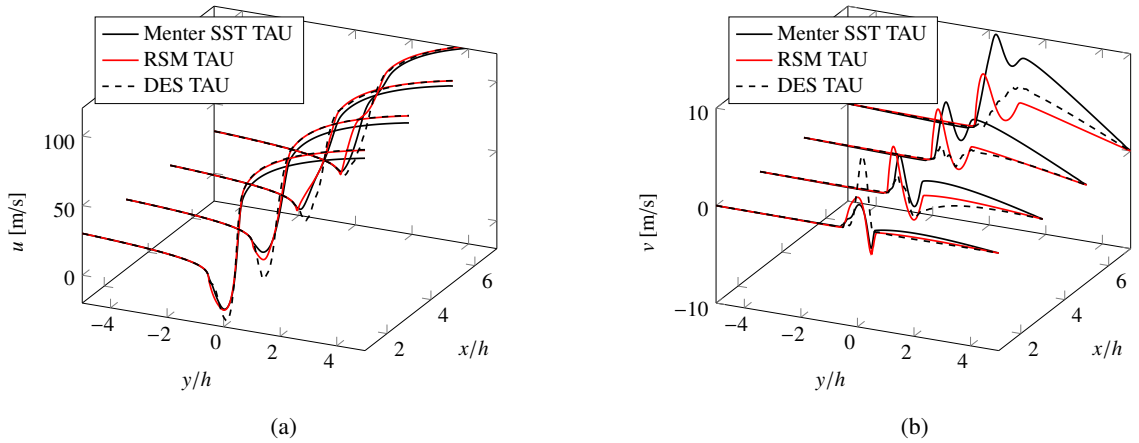

Figure 8: Transverse cuts of mean (a) axial velocity and (b) transverse velocity of the two-dimensional LOX/GH2 reacting case.

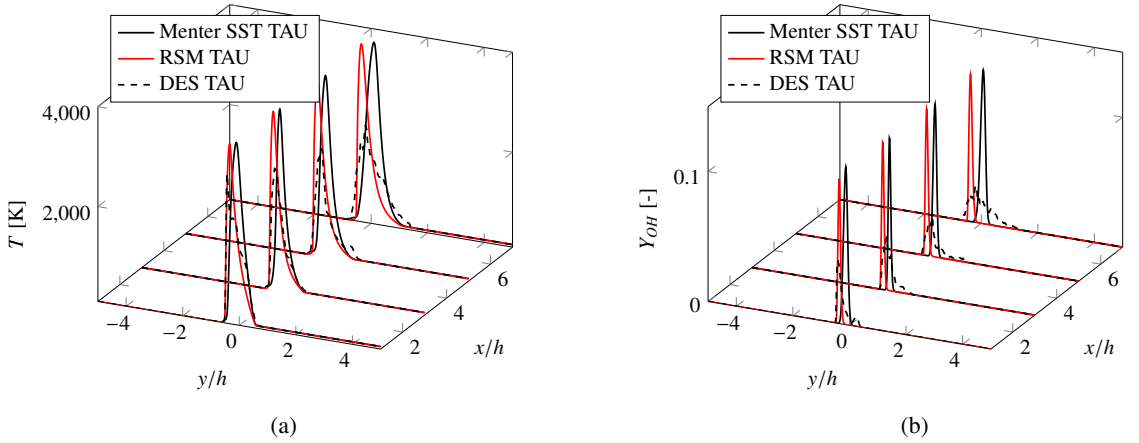

Figure 9: Transverse cuts of mean (a) temperature and (b) oxygen mass fraction of the two-dimensional LOX/GH2 reacting case.

3.2 Reacting test case

As a further extension of the previous transcritical mixing test case, we consider additionally the effect of chemical reactions onto the flow field. Thus, the hydrogen and oxygen are reacting and due to the exothermic reaction a (turbulent) hot flame zone is emerging. This additional zone changes the physics of the test case, as the flame zone is acting as a flow barrier between the two cryogenic fluids and prevents the excessive mixing between the hydrogen and oxygen layers. All other initial and boundary conditions as well as the mesh are unchanged. We use a finite-rate chemistry model using the simplified Jachimowski[12] (see table 1) reaction mechanism consisting of 6 species and 7 reactions. A visual plot of the instantaneous flow topology and the turbulent flame is shown in Figure 10. The statistical evaluation concerning the mean variables is shown in the Figures 8-9 at different cut-plane positions within the domain.

For this reacting case no quantitative mean results at several transverse cut positions are available in literature. Qualitatively the results are comparable to those presented by Ma[15] using a Flamelet model and those of Ruiz.[24] Due to the heat release and the resulting high temperatures in the chemical active zone, the flame separates the two almost pure component streams and suppresses the creation of large-scale vortical structures (compare Figures 3 and 10). This is in accordance with simulation results of Ruiz.[24]

Again the RANS turbulence models predict very well the velocity distribution at the transverse cuts in the flow domain with a smaller amplitude, similar to the previous mixing case. the RANS turbulence models overpredict the mean temperature and mean OH mass fraction. Furthermore, the position of the maximum mean temperature is only predicted correctly by the RSM turbulence model.

DOI: 10.13009/EUCASS2019-311

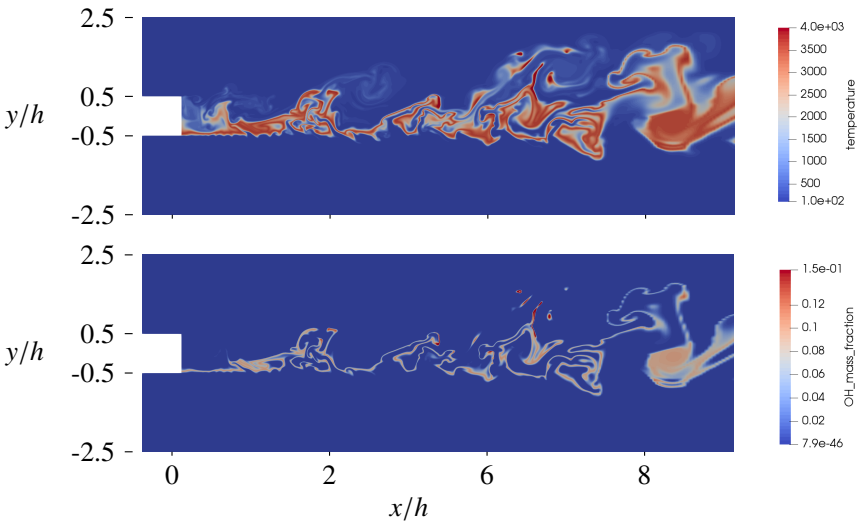

Figure 10: Instantaneous fields of temperature and OH mass fraction from top to bottom for the two-dimensional LOX/GH2 reacting case.

load step		3
$(O/F)_{injector}$	[-]	4
$(O/F)_{cc}$	[-]	1.32
$T_{inj,\,H2}$	[K]	158
$T_{inj,\,LOx}$	[K]	114
$v_{inj,\,H2}$	$[m/s]$	350
$v_{inj,\,LOx}$	$[m/s]$	30

Table 2: Measured test parameters taken from Suslov et al.[28]

	O/F_{cc} (O/F_{inj})	p [bar]
Experiment	1.1 (4)	60.9
SA		61.1

Table 3: Summary of the main experimental and numerical parameter

4. Comparison to BKC combustion chamber experiments

From this simple academic two-dimensional test case we move on to a more realistic sub-scale testbed configuration, the BKC single-injector combustion chamber at cryogenic conditions. The results in this part are work in progress, as we are working actively on the turbulence modeling at these conditions. Up to now we only have a comparison to the experimental results using the Spalart-Alamaras[26] turbulence model available.

In this comparison we consider a single-injector experiment, the DLR subscale thrust chamber model "C" (designated BKC) at the DLR test facility P8 in Lampoldshausen. The experimental results and boundary conditions are described by Suslov et al.[27,28] where an extensive description of the experimental test facility and the measurement techniques applied can be found. The experiments were designed to provide extended data for for high pressure LOx/GH2 combustion. Three different combustion chamber pressures from 40 to 60 bar were measured with three different oxidizer to fuel ratios (O/F) that cover the full range from sub- to supercritical combustion. We focus on the description of the numerical grid and boundary conditions and consider the supercritical load point with the shortest flame for a detailed comparison. At these conditions a supercritical combustion chamber of about 60 bar was measured.

4.1 Numerical domain and physical model

In this investigation we consider a two-dimensional axis-symmetric model for the flow in the single-injector combustion chamber. In Figure 11 a sketch of the two-dimensional axis-symmetrical computational domain is shown. The tubes of the injector are not modeled here and replaced by a stub tube with the respective experimental inflow conditions. The location of the boundary conditions is indicated in Figure 11, their values are given in the publication of Suslov et al.[28]

For this more complex comparison we just consider one RANS turbulence model, the one-equation Spalart-Alamaras model, that has provided robust solutions in under-resolved simulations. More complex RANS turbulence models are subject of further studies in this context.

DOI: 10.13009/EUCASS2019-311

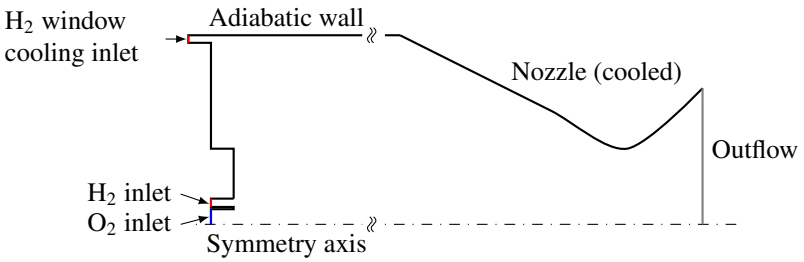

Figure 11: Sketch of the computational domain used in the numerical modeling (not to scale). The numerically chosen boundary conditions are indicated in the sketch.

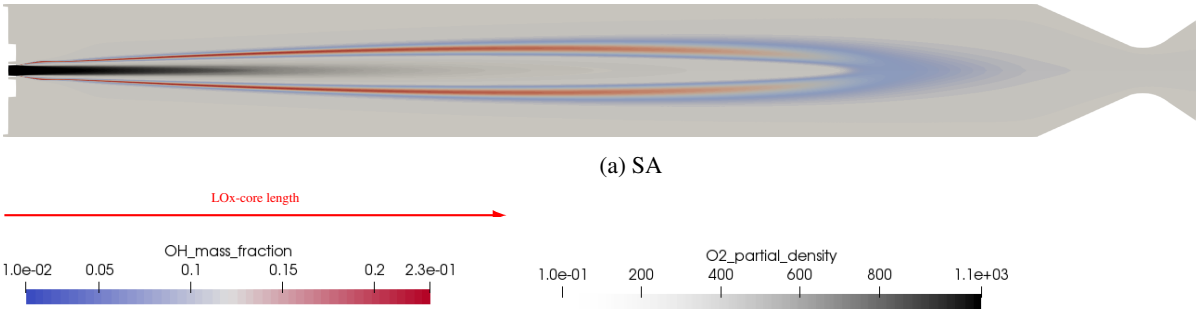

(a) SA

Figure 12: Comparison of flame structure and shadowgraph pictures

4.2 Flame structure

In Figure 12 we compare the structure of the flame within the combustion chamber. Additionally, we superimpose the density of the dense oxygen core as it would appear on shadowgraph images based on the density field. An arrow indicates the experimentally measured length of the LOx core based on the half intensity criterion (see Suslov et al.[28] for more information). Even with the simple SA turbulence model, that is known to be dissipative for jets, we are able to obtain suitable flame and LOx-core lengths.

4.3 Wall temperature and pressure measurements

In the experimental measurement the pressure and temperature distribution at the combustor walls were measured using pressure and temperature transducers. Due to the fact that data points from different test runs are combined, that is needed to be able to change the window position to provide optical access of the whole combustion chamber, the scatter in the experimental data is quite large. In Figure 13 the numerical and experimental wall pressures and temperatures are compared to the numerical results.

The wall pressure distribution shown in Figure 13 (a) fitting with an accuracy of less than 1 % of the average experimental wall pressure.

The wall temperature distribution (see Figure 13 (b)) is well predicted by the numerical models and fits very well to the experimentally measured values. However, it should be noted that in this combustion chamber with excessive window cooling, the wall temperature distribution is dominated by the window cooling massflow. This additional injection is needed to prevent a failing of the optical access windows.

5. Conclusion

In this paper we have shown the application of different RANS turbulence models to compressible cryogenic flows, that for example can be encountered in rocket combustion chambers. We have investigated three different test cases ranging from the simple academic Ruiz test case for which detailed turbulent statistics are available to a more complex single-injector subscale combustion chamber.

For the Ruiz test case the agreement between the DES and the RANS approaches is very good, even though the transient mixing processes can not be resolved by the steady RANS methods. The averaged statistics fit very well but show slight differences because a 2D RANS simulation provides physical turbulence results while a 2D DES/LES

DOI: 10.13009/EUCASS2019-311

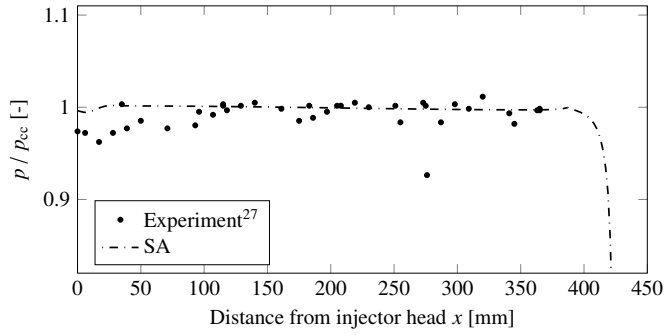

(a) Pressure

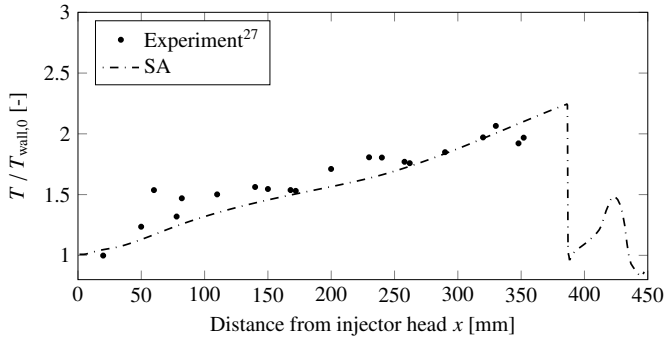

(b) Temperature

Figure 13: Comparison of wall pressure and temperature measurements.

provides unphysical results. For the case with combustion effects this global perspective does not change. In the application test case of the subscale rocket combustion chamber BKC we have only applied the Spalart-Alamaras turbulence model for now, that is known to be too dissipative for jet flows. In further studies the effect of the turbulence model onto the much lower resolved case within rocket combustion chambers has to be investigated. Another key parameter would be to include an advanced combustion modeling based on presumed probability density function based approaches as well as the use of flamelet methods.

6. Acknowledgments

The present work was conducted in the framework of the German Aerospace Center (DLR) project TAUROS (TAU for Rocket Thrust Chamber Simulation) focusing on the qualification and advancement of the DLR flow solver TAU for liquid rocket thrust chamber applications. The financial support of the DLR Space Research Programmatic is highly appreciated.

A. Cryogenic fluid model

The cryogenic fluid behavior is modeled by a standard generalized cubic EOS (for a summary see e. g. Kim et al.,[14] Hsieh & Yang[11]) that is described as

$$p = \frac{\rho R_u T}{M_w - b\rho} - \frac{a\alpha(T)\rho^2}{(M_w + \delta_1 b\rho)(M_w + \delta_2 b\rho)} \tag{3}$$

DOI: 10.13009/EUCASS2019-311

with the cubic EOS mixture coefficients

$$a\alpha = \sum_{i=1}^{N}\sum_{j=1}^{N} X_i X_j a_{ij}\alpha_{ij} \tag{4}$$

$$b = \sum_{i=1}^{N} X_i b_i \tag{5}$$

$$\delta_1 = \sum_{i=1}^{N} X_i \delta_{1,i} \tag{6}$$

$$\delta_2 = \sum_{i=1}^{N} X_i \delta_{2,i} \tag{7}$$

for N number of species in the mixture. The X_i are the species mole fractions. The parameters δ_1 and δ_2 is a switching parameter for a family of cubic EOS. For the Peng-Robinson EOS, $\delta_1 = 1 + \sqrt{2}$ and $\delta_3 = 1 - \sqrt{2}$. For each species the attraction factors a_i and α_i as well as volume correction term b_i are calculated from the species critical conditions.

The mixture attraction factor $a_{ij}\alpha_{ij}$ is calculated according a combination rule

$$a_{ij}\alpha_{ij} = \sqrt{a_i a_j \alpha_i \alpha_j}(1 - k_{ij}) \tag{8}$$

$$\frac{\partial a_{ij}\alpha_{ij}}{\partial T} = 0.5\sqrt{a_i a_j}\left[\sqrt{\frac{\alpha_i}{\alpha_j}}\frac{\partial \alpha_j}{\partial T} + \sqrt{\frac{\alpha_j}{\alpha_i}}\frac{\partial \alpha_i}{\partial T}\right] \tag{9}$$

$$\frac{\partial^2 a_{ij}\alpha_{ij}}{\partial T^2} = \sqrt{a_i a_j}\left[\frac{1}{2\sqrt{\alpha_i\alpha_j}}\frac{\partial \alpha_i}{\partial T}\frac{\partial \alpha_j}{\partial T} - \frac{1}{4}\sqrt{\frac{\alpha_i}{\alpha_j^3}}\left(\frac{\partial \alpha_j}{\partial T}\right)^2 - \frac{1}{4}\sqrt{\frac{\alpha_j}{\alpha_i^3}}\left(\frac{\partial \alpha_i}{\partial T}\right)^2\right. \tag{10}$$

$$\left. + \frac{1}{2}\sqrt{\frac{\alpha_i}{\alpha_j}}\frac{\partial^2 \alpha_j}{\partial T^2} + \frac{1}{2}\sqrt{\frac{\alpha_j}{\alpha_i}}\frac{\partial^2 \alpha_i}{\partial T^2}\right] \tag{11}$$

with k_{ij} being an empirical binary interaction parameter for the mixture. For the current implementation this parameter is set to zero.

References

[1] Rémi Abgrall and Smadar Karni. Computations of compressible multifluids. *Journal of Computational Physics*, 169(2):594–623, 2001.

[2] Daniel T Banuti, Volker Hannemann, Klaus Hannemann, and Bernhard Weigand. An efficient multi-fluid-mixing model for real gas reacting flows in liquid propellant rocket engines. *Combustion and Flame*, 168:98–112, 2016.

[3] Daniel T Banuti, Peter C Ma, Jean-Pierre Hickey, and Matthias Ihme. Thermodynamic structure of supercritical lox–gh2 diffusion flames. *Combustion and Flame*, 196:364–376, 2018.

[4] Josette Bellan. Supercritical (and subcritical) fluid behavior and modeling: drops, streams, shear and mixing layers, jets and sprays. *Progress in energy and combustion science*, 26(4):329–366, 2000.

[5] G Billet and R Abgrall. An adaptive shock-capturing algorithm for solving unsteady reactive flows. *Computers & fluids*, 32(10):1473–1495, 2003.

[6] Michael Dumbser, Uwe Iben, and Claus-Dieter Munz. Efficient implementation of high order unstructured WENO schemes for cavitating flows. *Computers & Fluids*, 86:141–168, 2013.

[7] Stefan Fechter, Tim Horchler, Sebastian Karl, and Klaus Hannemann. Efficient handling of cryogenic equation of state for the simulation of rocket combustion chambers. In *2ND INTERNATIONAL SEMINAR ON NON-IDEAL COMPRESSIBLE-FLUID DYNAMICS FOR PROPULSION & POWER*. Springer, 2018.

[8] Peter Gerlinger. *Numerische Verbrennungssimulation: Effiziente numerische Simulation turbulenter Verbrennung*. Springer-Verlag, 2005.

[9] Peter Gerlinger, Helge Möbus, and Dieter Brüggemann. An implicit multigrid method for turbulent combustion. *Journal of Computational Physics*, 167(2):247–276, 2001.

DOI: 10.13009/EUCASS2019-311

[10] Volker Hannemann. *Numerische Simulation von Stoß-Stoß-Wechselwirkungen unter Berücksichtigung von chemischen und thermischen Nichtgleichgewichtseffekten*. PhD thesis, 1997.

[11] Shih-Yang Hsieh and Vigor Yang. A preconditioned flux-differencing scheme for chemically reacting flows at all mach numbers. *International Journal of Computational Fluid Dynamics*, 8(1):31–49, 1997.

[12] Casimir J Jachimowski. An analytical study of the hydrogen-air reaction mechanism with application to scramjet combustion. 1988.

[13] Sebastian Karl. *Numerical investigation of a generic scramjet configuration*. PhD thesis, University of Dresden, 2011.

[14] Seong-Ku Kim, Hwan-Seok Choi, and Yongmo Kim. Thermodynamic modeling based on a generalized cubic equation of state for kerosene/lox rocket combustion. *Combustion and Flame*, 159(3):1351–1365, 2012.

[15] Peter C. Ma. *MODELING OF TURBULENT MIXING AND COMBUSTION AT TRANSCRITICAL CONDITIONS*. PhD thesis, Stanford University, 2018.

[16] Peter C Ma, Yu Lv, and Matthias Ihme. An entropy-stable hybrid scheme for simulations of transcritical real-fluid flows. *Journal of Computational Physics*, 340:330–357, 2017.

[17] Florian R Menter. Two-equation eddy-viscosity turbulence models for engineering applications. *AIAA journal*, 32(8):1598–1605, 1994.

[18] F.R. Menter, M. Kuntz, and R. Langtry. Ten years of industrial experience with the SST turbulence model. In K. Hanjalić, Y. Nagano, and M. Tummers, editors, *Turbulence, Heat and Mass Transfer 4*, Conference Proceeding Series, pages 625–632. 2003.

[19] Joseph C Oefelein. Thermophysical characteristics of shear-coaxial lox–h_2 flames at supercritical pressure. *Proceedings of the Combustion Institute*, 30(2):2929–2937, 2005.

[20] André Péneloux, Evelyne Rauzy, and Richard Fréze. A consistent correction for Redlich-Kwong-Soave volumes. *Fluid Phase Equilibria*, 8(1):7–23, 1982.

[21] Ding-Yu Peng and Donald B Robinson. A new two-constant equation of state. *Industrial & Engineering Chemistry Fundamentals*, 15(1):59–64, 1976.

[22] Bruce E. Poling, John M. Prausnitz, and John P. O'Connel. *The properties of gases and liquids*. McGraw Hill Book Co., New York, NY, 5th edition edition, 2007.

[23] Cord-Christian Rossow. Extension of a compressible code toward the incompressible limit. *AIAA journal*, 41(12):2379–2386, 2003.

[24] Anthony Ruiz. *Unsteady numerical simulations of transcritical turbulent combustion in liquid rocket engines*. PhD thesis, Institut Nationale Polytechnique de Toulouse, 2012.

[25] Anthony M Ruiz, Guilhem Lacaze, Joseph C Oefelein, Raphael Mari, Bénédicte Cuenot, Laurent Selle, and Thierry Poinsot. Numerical benchmark for high-reynolds-number supercritical flows with large density gradients. *AIAA Journal*, 2015.

[26] Philipe R Spalart and Stephen R Allmaras. A one equation turbulence model for aerodynamic flows. *AIAA journal*, 94, 1992.

[27] Dmitry I Suslov, Justin S Hardi, Bernhard Knapp, and Michael Oschwald. Hot-fire testing of liquid oxygen/hydrogen single coaxial injector at high-pressure conditions with optical diagnostics. *Progress in Propulsion Physics*, 11:391–406, 2019.

[28] Dmitry I Suslov, Justin S Hardi, and Michael Oschwald. Full-length visualisation of liquid oxygen disintegration in a single injector sub-scale rocket combustor. *Aerospace Science and Technology*, 2019.

[29] David C Wilcox et al. *Turbulence modeling for CFD*, volume 2. DCW industries La Canada, CA, 1998.